Glacial-Geologic Evidence for Decreased Precipitation During The Little Ice Age in The Brooks Range, Alaska

Authors: Sikorski, Janelle J., Kaufman, Darrell S., Manley, William F., and Nolan, Matt

Source: Arctic, Antarctic, and Alpine Research, 41(1) : 138-150

Published By: Institute of Arctic and Alpine Research (INSTAAR), University of Colorado

URL: https://doi.org/10.1657/1523-0430-41.1.138

Arctic, Antarctic, and Alpine Research, Vol. 41, No. 1, 2009, pp. 138–150

Glacial-Geologic Evidence for Decreased Precipitation during the Little Ice Age in the Brooks Range, Alaska

Janelle J. Sikorski§*
Darrell S. Kaufman¶*
William F. Manley† and
Matt Nolan‡

*Department of Geology, Northern Arizona University, Flagstaff, Arizona 86011, U.S.A.
†Institute of Arctic and Alpine Research, University of Colorado, Boulder, Colorado 80309, U.S.A.
‡Institute of Northern Engineering, University of Alaska Fairbanks, Alaska 99775, U.S.A.
§Present address: Department of Geology, Miami University, Oxford, Ohio 45056
¶Corresponding author: darrell.kaufman@nau.edu

Abstract

We mapped Little Ice Age (LIA) moraines in the Brooks Range to estimate former equilibrium-line altitudes (ELAs), and combined this information with available proxy temperature estimates to infer precipitation trends because little is known about precipitation changes associated with centennial-scale climate variability in the Arctic during the late Holocene. The Brooks Range, northern Alaska (68°N), hosts hundreds of extant glaciers that exhibit geomorphic evidence for multiple fluctuations in ice extent during the past millennium. Our lichenometric age estimates for LIA moraines in the forefields of five cirque glaciers in the Sagavinerktok River valley and Oolah Valley suggest two intervals of LIA moraine formation centered around A.D. 1250 and 1650. The outermost LIA moraine was mapped on aerial photographs for 114 relatively large (1.2 ± 0.5 km) and geographically simple glaciers along a 700-km-long transect following the range crest. At their maximum extent during the LIA, these glaciers were an average of 0.2 ± 0.1 km longer than the ice margins shown on most recent U.S. Geological Survey topographic maps (1956 and 1972). The ELA was estimated using an accumulation-area-ratio method and GIS analysis. The reconstructed ELAs needed to maintain an equilibrium length for the LIA glaciers were an average of 51 ± 29 m lower than for the smaller glacier sizes of the mid 20th century. This small ELA lowering during the LIA is less than would be expected from available proxy temperature estimates from elsewhere in Alaska that indicate warm-season temperature reductions of about 1 °C. To explain this discrepancy, we suggest that precipitation decreased during the LIA. A prolonged southern displacement of the Arctic front might explain the drier conditions in the Brooks Range during the LIA.

DOI: 10.1657/1938-4246(07-078)[SIKORSKI]2.0.CO;2

Introduction

The Little Ice Age (LIA) is widely recognized as the most recent period of Neoglacial cooling, and it attests to the tendency of Earth's climate to change appreciably on time scales of decades to centuries. Multiple lines of historical and proxy climate evidence suggest that northern hemisphere summer temperatures were on average about 0.5 to 1.0 °C lower during the LIA than the 20th century (e.g., Moberg et al., 2005), although the spatial variability of cooling was high (e.g., D'Arrigo et al., 2006), and temperature changes at high latitudes seemed to have exceeded the global average (Overpeck et al., 1997). Less is known about precipitation changes during the LIA, especially at high latitudes, despite the importance of moisture availability to a broad range of physical and biological processes in the Arctic (Mann et al., 2002a; Nesje and Dahl, 2003). This study provides a quantitative comparison of glacier extent between the LIA and the mid 20th century in the Brooks Range of arctic Alaska, and furthers our understanding of precipitation dynamics prior to the advent of instrumental weather data in this region.

Land-based glaciers expand and retreat in response to changes in mass balance largely controlled by climate. Such fluctuations are often cited as prima facie evidence for climate change (e.g., Lowell, 2000; Oerlemans, 2005). A climatically meaningful measure of glacier extent is the equilibrium-line altitude (ELA), which is controlled mainly by the counterbalancing influences of warm-season melting and cold-season accumulation. During years of positive annual balance, the ELA of a glacier lowers, and the glacier tends towards advancing until its size comes into equilibrium with the new climate and the mass balance is once again zero. If the ice marginal position is sustained, a moraine can form. Reconstructions of ELAs based on moraine positions provide information about climate variations in the past, including during the LIA (e.g., Dahl and Nesje, 1992, 1996).

The polythermal glaciers of the Brooks Range, Alaska (Fig. 1), are particularly sensitive to climate change because they are located in a relatively arid environment, where mass flux is low and mass balance is highly responsive to summer ablation (Calkin et al., 1985). In this study, we estimate the ELA of glaciers for both the mid 20th century and the LIA maximum in the Brooks Range. Our ELA reconstructions coupled with previously published LIA summer temperature reconstructions for northern Alaska suggest that, during the LIA maximum, glaciers expanded under drier conditions.

Setting

The Brooks Range is located between the North Slope and Yukon Basin of Alaska, and extends from the Chukchi Sea to the

1523-0430/09 $7.00

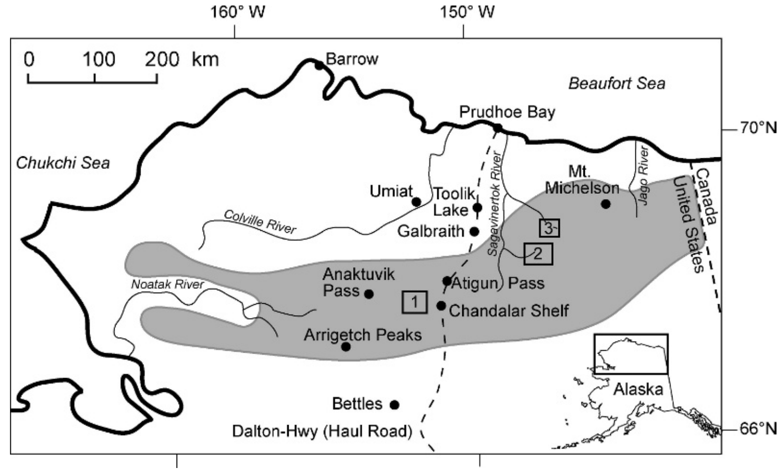

FIGURE 1. Northern Alaska showing extent of the Brooks Range (gray) and the three areas where moraines were mapped in the field (black boxes; [1] = Oolah Valley, [2] = Sagavinertok River valley, and [3] = Accomplishment Creek valley).

Alaska-Yukon border, spanning from 141° to 163°W at 68°N (Fig. 1). The mountains increase in elevation eastward, with summits reaching ~2700 m a.s.l. On the basis of our analysis of topographic maps by the U.S. Geological Survey, the Brooks Range supports over 800 modern cirque and small valley glaciers (most <1 km long). In this paper, "modern" refers to the glacier positions delimited on 1:63,360-scale topographic maps, which are based on aerial photographs taken in 1970 and 1955 of the central and northeastern Brooks Range, respectively. The largest glaciers (up to 10 km long) are located in the northeastern Brooks Range, where glaciation thresholds are the highest (Porter et al., 1983; Balascio et al., 2005). In general, glaciers are located in north-facing cirques that were formed by more extensive glaciers that covered most of the central and eastern Brooks Range during repeated Pleistocene glaciations (Hamilton, 1986).

Glacier fluctuations during the Holocene are relatively well documented in the Brooks Range. Early work by Detterman et al. (1958), Porter and Denton (1967), and others resulted in a general framework of middle and late Holocene advances. More recent research (Ellis and Calkin, 1979, 1984; Calkin and Ellis, 1980; Ellis et al., 1981; Calkin et al., 1985) based on extensive mapping and lichenometric analysis supports the conclusions of earlier studies that the glaciers of the Brooks Range advanced several times throughout the Neoglaciation. A few historical records, including those of Leffingwell (1919), have been used to constrain the age of LIA moraines in the Brooks Range (Evison et al., 1996). This study expands on the detailed Holocene moraine mapping available for the central Brooks Range.

Weather stations are sparse and unevenly distributed across the Brooks Range. Most of the stations in northern Alaska are at low-elevation sites, such as in river valleys and along the coast of the Arctic Ocean. Mean annual temperatures for the Brooks Range are between −4 and −12 °C (http://prism.oregonstate.edu/state_products/ak_maps.phtml), and decrease toward the Chukchi and Beaufort Seas. Ablation-season (JJA) temperatures at McCall Glacier, among the highest glaciers in the range, averaged about 2 °C during 1957–1958 (Orvig, 1961). More recent measurements show that average summer temperatures can exceed 5 °C in some years on McCall Glacier (Klok et al., 2006). The glaciers of the Brooks Range receive most of their moisture from the Pacific Ocean (Porter et al., 1983), although the Arctic Ocean provides moisture to some of the glaciers in the northernmost part of the range (Rabus and Echelmeyer, 1998; Matt Nolan, unpublished). Precipitation receipts in the Brooks Range are poorly documented. The smoothed circum-arctic representation of Serreze and Hurst (2000) shows average annual precipitation over the Brooks Range of around 300 mm. The more spatially refined PRISM model for Alaska generally shows similar values, but the modeled precipitation increases with elevation in the Brooks Range, reaching around 600 mm over the crest of the range where the study glaciers are located (http://prism.oregonstate.edu/state_products/ak_maps.phtml).

Methods

MORAINE MAPPING

The glaciers selected for this study are located along a 700-km-long transect that follows the central divide of the Brooks Range. The sample set of 114 glaciers includes some of the largest in the range; they average 1.2 ± 0.5 km long and 0.6 ± 0.5 km^2 in area (Table 1; Appendix). Together, they comprise 13% of the total "modern" glacier area in the Brooks Range, with an area-altitude distribution representative of the aggregate glaciated area (Fig. 2). Most glaciers are confined to the highest cirques along the range crest where their mean elevation averages 1810 ± 180 m a.s.l. From west to east, this transect includes 15 glaciers around the Arrigetch Peaks, nine around Anaktuvuk Pass, 65 in the Atigun Pass area, and 24 glaciers from the Mount Michelson area. The spatial density of this data set is 1.0 glacier per 1000 km^2 in an area of 115,000 km^2. This sample population is biased toward the larger glaciers located close to the range crest. It might underestimate the broader population of glaciers that includes numerous smaller (<0.5 km), isolated glaciers far to the north and south of the range crest, and glaciers located in compound cirques with complex accumulation areas. We also avoided glaciers with extensive debris cover.

The maximum extent reached by these 114 glaciers during the LIA was mapped on the basis of glacial morphological evidence interpreted from 1:70,000-scale aerial photographs taken in 1955 (eastern Brooks Range) and 1970 (central Brooks Range) (Sikorski, 2004). In general, all LIA moraines lack vegetation cover, have well-defined moraine crests, and are a short distance down valley (≤1.5 km) from "modern" glaciers (Fig. 3). Seven glaciers within three valleys in the central Brooks Range were chosen to field-check our aerial photograph interpretation. From west to east these are located in the Oolah Valley, Sagavinertok River valley, and Accomplishment Creek valley; all are northward flowing (Fig. 1). They are distributed along a 90-km-long segment of the continental divide and are located in six predominately north-facing cirques (aspect = 330 to 15°) between 1800 and 2300 m a.s.l. The forefields of these glaciers were not studied by

TABLE 1

Summary statistics (mean ± 1σ) for physical parameters and estimated equilibrium-line altitudes (ELAs) for Brooks Range glaciers.

Parameter	Modern[a]			Little Ice Age		
	Central	Northeastern	Combined	Central	Northeastern	Combined
Average length (km)	1.1 ± 0.5	1.4 ± 0.7	1.2 ± 0.5	1.3 ± 0.5	1.7 ± 0.7	1.4 ± 0.6
Average area (km^2)	0.6 ± 0.4	0.8 ± 0.8	0.6 ± 0.5	0.7 ± 0.5	1.2 ± 0.9	0.8 ± 0.6
Average ELA (m)[b]	1766 ± 149	2027 ± 95	1816 ± 184	1713 ± 145	1977 ± 102	1776 ± 173
Number of glaciers analyzed	90	24	114	90	24	114

[a] 'Modern' refers to glacier positions delimited on U.S. Geological Survey topographic maps, which are based on aerial photographs taken in 1970 and 1955 of the central and northeastern Brooks Range, respectively.

[b] Modern ELA based on accumulation area ratio (AAR) of 0.48; LIA ELA based on AAR of 0.58.

Ellis and Calkin (1984), and they have not previously been mapped in more detail than 1:250,000 (Hamilton, 1979, 1981). These glaciers were chosen because they (1) showed clear Neoglacial moraines in the aerial photographs, (2) are well distributed along the southwest-northeast–trending range crest, and (3) have clear accumulation areas that are confined to simple cirques.

LICHENOMETRY

We used lichenometry to estimate the ages of moraines mapped in the field. We focused on the lichen genus *Rhizocarpon* because of its slow and regular growth rate, ubiquity, and ease of recognition. Its yellow-green color distinguishes the genus, but identification of individual species is difficult (Innes, 1985). Therefore, our measurements might include several species (e.g., *R. superficiale*, *R. eupetraeoides*, and *R. inarense*—referred to here collectively as *R. sensu lato*). Following the procedure used by Calkin and Ellis (1980) to develop the lichen growth curve for the Brooks Range, we relied on the maximum thallus diameter of the largest lichen to characterize each moraine. This approach assumes that the diameter of the single largest lichen is the best indicator of substrate age because it was the first to colonize. The diameters of the five largest lichens on each moraine were tabulated by Sikorski (2004). The average values of the five largest are about 10% smaller than the single largest, and the size groups are more tightly clustered, suggesting average values are a

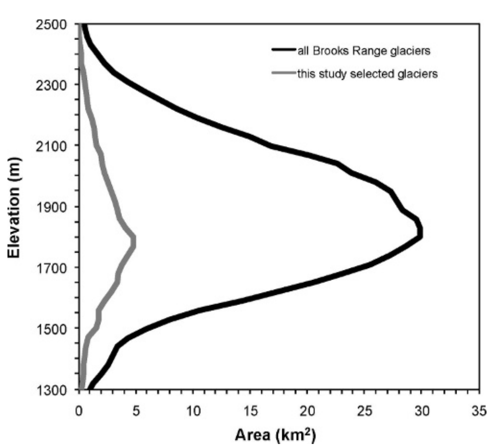

FIGURE 2. Area-altitude distribution of glaciers in the Brooks Range based on U.S. Geological Survey topographic maps (1970 and 1950 for the central and eastern Brooks Range, respectively). Black line is aggregate of all glaciers; gray line represents the 114 glaciers used in this study. Elevation bin size is 30 m.

more sound chronologic index, assuming that the ages of the moraines should cluster in discrete groups. To measure lichen, we walked along the entire length of each moraine crest and measured the diameter of the longest axis of large lichen to the nearest millimeter using a digital caliper. Only lichens that were slightly elliptical to circular with discrete thalli were included. For moraine ridges longer than about 50 m, we established several stations and recorded lichen sizes within a 10 m radius of each station.

The original lichen growth curve for the central Brooks Range (Calkin and Ellis, 1980) was recently updated by Solomina and Calkin (2003). Their *R. geographicum s.l.* growth curve is constrained by 12 lichen diameters ranging from 2 to 50 mm from surfaces between 20 and 1260 L yr (where "L yr" is lichenometric age relative to A.D. 1950) (Fig. 4). We fit a least-squares second-order polynomial to the published lichen-growth calibration data (Solomina and Calkin, 2003) and specified a y-intercept of 30 yr to incorporate the estimated colonization time for *R. geographicum s.l.* (Calkin and Ellis, 1980). The age equation is:

$$y = 0.4227x^2 + 4.25x + 30 \ (R^2 = 0.96, p < 0.01) \qquad (1)$$

where x is the lichen diameter in mm, and y is age in L yr. In addition to incorporating colonization time, this equation yields younger and possibly more realistic ages for lichens older than about 2000 L yr compared to the logarithmic model proposed by Solomina and Calkin (2003). We used this equation to estimate ages for Neoglacial moraines with lichens up to 150 mm in diameter.

The ages of lichens larger than 50 mm are uncertain because they fall beyond the range of the calibration points and are therefore dependent on the choice of curve-fit model used to extrapolate lichen ages. We consider the ±20% error in lichen ages used by Calkin and Ellis (1980) to be a reasonable estimate. This error incorporates the uncertainty associated with locating the single largest lichen on a moraine, the influence of moraine lithology and variable stabilization times on lichen size, and microclimate variations that control lichen growth. This level of certainty is sufficient for the purposes of this study.

ELA RECONSTRUCTIONS

The ELA of a glacier typically undergoes significant variation from year to year in response to variable weather patterns. These annual variations rarely leave lasting geomorphic evidence. In contrast, reconstructing the ELAs of paleoglaciers relies on geomorphic evidence for relatively stable ice-marginal positions. It is assumed that they represent "steady-state" conditions during which a glacier maintains a particular geometry long enough to build a significant moraine (e.g., Seltzer, 1994). During this

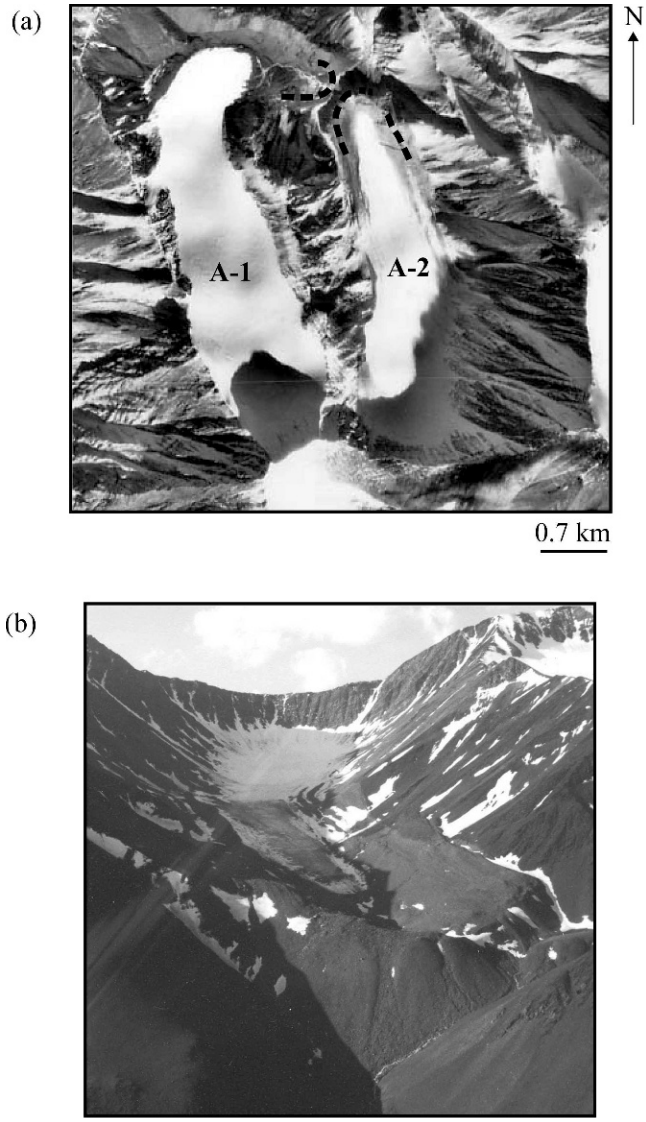

FIGURE 3. Typical central Brooks Range glaciers and associated Little Ice Age (LIA) moraines. Glaciers are flowing toward the north. (a) Aerial photograph of two glaciers located in the headwaters of Accomplishment Creek in 1970. The inferred LIA maximum extents of these glaciers are highlighted (dashed lines). (b) Aerial view looking south toward glacier A-2. Photograph taken in July 2003. LIA moraines have well-defined moraine crests and lack vegetation.

interval of relative stability, the typical annual net mass balance is zero, and the glacier geometry is in equilibrium with the climate.

A variety of methods have been used to reconstruct steady-state ELAs of paleoglaciers (recently reviewed by Benn et al., 2005). We used the accumulation area ratio (AAR) method, which has been shown to produce consistent results, especially for glaciers with simple geometries like those in this study. This method is based on glacier extent depicted on maps or reconstructed from ice-marginal geomorphic features, and it assumes a fixed ratio between the accumulation and ablation area of a glacier. AAR values for alpine glaciers with long-term mass-balance measures typically range from 0.55 to 0.65 globally (Dyurgerov, 2002). For the reconstructed LIA glaciers, we assumed an AAR of 0.58, which is the average value for the interpolated steady-state mass balance of alpine glaciers in Dyurgerov's (2002) global data set (Dyurgerov, personal communication to W. F. Manley). The actual value depends on a variety

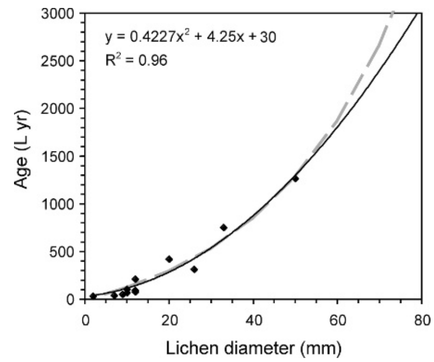

FIGURE 4. Lichen growth curve for the central Brooks Range used to date moraines in this study. Data of Solomina and Calkin (2003) were fit to a least-squares second-order polynomial (curved line). The growth curve preferred by Solomina and Calkin (2003) uses a logarithmic fit (dashed line), which yields older extrapolated ages for lichens beyond 2000 L yr.

of factors, but because we are primarily concerned with the difference between ELAs inferred for the "modern" and the LIA maximum ice extents (ΔELA), our analysis is largely insensitive to the choice of AAR value. In this sense, ELA serves as an index of glacier extent, similar to the glacier median altitude. ΔELA does, however, depend on whether the AAR was the same for both the "modern" and LIA glaciers. Glaciers shown on U.S. Geological Survey topographic maps were in various states of retreat from their LIA maxima. Their geometry reflects cumulative mass balance during the few decades (estimated response time) prior to 1955 and 1970, and the AAR of a retreating glacier is less than for its steady state, LIA counterpart. For "modern" glaciers, we used an AAR of 0.48, which is based on data from McCall Glacier, the only glacier monitored regularly for mass balance in northern Alaska. The mass balance of the glacier was measured annually between 1969 and 1972, and the long-term average balance was calculated using surface-elevation surveys for the interval between 1958 and 1971 (Rabus and Echelmeyer, 1998). These results converge on an AAR of about 0.48 for the interval prior to the rapid retreat of recent decades.

ELAs were determined using geographic information system (GIS) techniques. Briefly, "modern" and reconstructed LIA maximum extents were delimited on 1:63,360-scale maps, then digitized in GIS. Elevations were assigned to the glacier outlines based on the digital elevation models (DEM) with a grid resolution of 60 m (USGS National Elevation Dataset). The hypsometry of the glacier surface was assessed at 3-m-elevation increments. U.S. Geological Survey standards for the DEMs used in this analysis have root mean squared errors of 10–15 m, one half of the contour interval (U.S. Geological Survey, 1998).

Results and Comparison with Other Studies

RECONSTRUCTION OF LIA GLACIERS AND LICHENOMETIC AGES

Lichenometric ages were estimated at 24 lichen stations or transects, most on individual moraines in the forefields of the five glaciers that we studied in the Sagavinertok River valley and Oolah Valley (Fig. 5). We excluded the results from the forefields of the two glaciers studied in the Accomplishment Creek valley because the shale-dominated, unstable moraine crests in this valley had few boulders with lichens. Maximum lichen diameters range broadly from 10 to 106 mm and systematic patterns are difficult to infer from our small data set. Overall, lichen sizes generally

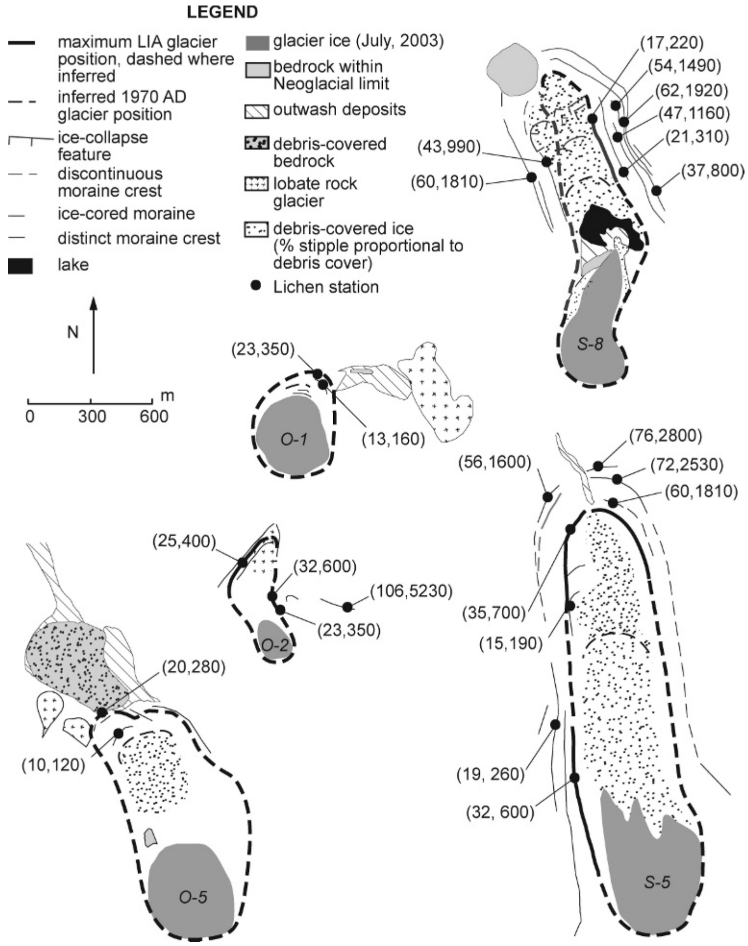

FIGURE 5. Maps of Holocene moraines and outwash fronting five of the seven glaciers studied in the central Brooks Range. Numbers in parentheses are the single largest lichen (mm) measured on the moraine followed by its lichenometric age estimate (L yr). The transition between debris-covered glacier and rock glacier is gradational, and all debris-covered ice was mapped as a single unit. The down-slope increase in debris cover may mark the transition. Locations of glaciers as follows: O1: 68.110°N, 150.474°W; O2: 68.033°N, 150.401°W; O5: 68.036°N, 150.172°W; S5: 68.266°N, 148.451°W; S8: 68.315°N, 148.337°W.

increase with distance from the ice margin. Reversals in down-valley trends tend to be located at stations near the up-valley extent of lateral moraines, where slope stability or lichen die-off under perennial snow might be a factor. In general, the distribution of lichen sizes shows a break between about 35 and 50 mm, with only one (up-valley) station with maximum lichen sizes within this gap. This gap corresponds to ages of about 1300 to 700 L yr (A.D. 650 to 1250). Moraines with lichens larger than about 50 mm predate the LIA. They tend to have noticeably more subdued ridges, stable frontal slopes, some sod cover, and lichen-encrusted boulders, all of which can be recognized on aerial photographs. We used this break in weathering and lichen characteristics to delimit the LIA maximum advance in glacier forefields that were not studied on the ground.

Older Neoglacial moraines that predate the LIA are present at most glaciers in the Brooks Range, where they record advances that extended several hundred meters beyond the LIA margin. At the five glaciers where lichenometry could be used, lichen diameters typically range between 50 and 70 mm on these moraine ridges, indicating ages of around 1800 ± 500 L yr. These ages are consistent with ages of other Neoglacial moraines from elsewhere in the central Brooks Range reported by Ellis and Calkin (1984). Lichen diameters of >100 mm on one moraine located 0.3 km beyond the LIA margin at glacier O-2 indicate a much older Neoglacial advance during the mid-Holocene, as has been discussed previously for elsewhere in the Brooks Range (e.g., Calkin and Ellis, 1980).

The outermost LIA moraines at the five glacier forefields studied in the field have maximum lichen diameters that range between 17 and 35 mm (Fig. 5). Four of the five fall within the narrow range of 21 ± 4 mm, which equates to an average age of 320 ± 80 L yr (A.D. 1550 to 1710), and the fifth is about twice as old (700 L yr = A.D. 1250). Although our sample size is small, the frequency distribution of lichen ages at all stations indicates two phases of moraine stabilization during the last millennium (Fig. 6). The earlier period of moraine stabilization occurred around 700 L yr (A.D. 1250), and the more recent around 300 L yr (A.D. 1650), as evidenced by modes in the frequency distribution. Although the data are sparse, they agree with the results of the more extensive study of Ellis and Calkin (1984) who concluded that the LIA maximum in the Brooks Range was reached between A.D. 1250 and 1650. These correspond with the Maunder and Wolf minima in solar irradiance, providing further evidence that glaciers fluctuations on centennial time scales are associated with solar variability in Alaska (Wiles et al., 2004) and elsewhere (e.g., Luckman and Wilson, 2005; Polissar et al., 2006).

LITTLE ICE AGE ELAs

The maximum extent of glaciers during the LIA seems to have been reached at different times at different glaciers, but the lichenometric results lend confidence to our ability to distinguish between LIA maximum and older Neoglacial moraines based on the interpretation of similar features on aerial photographs from other valleys. On average, during the LIA maximum, the 114 glaciers that we mapped on aerial photographs lengthened by 0.2 ± 0.1 km and gained 0.14 ± 0.03 km^2 compared to their "modern" positions (Table 1; Appendix). On the basis of these paleoglacier reconstructions, and using an AAR of 0.58, the ELAs of reconstructed LIA glaciers increase from 1450 ± 95 m in the

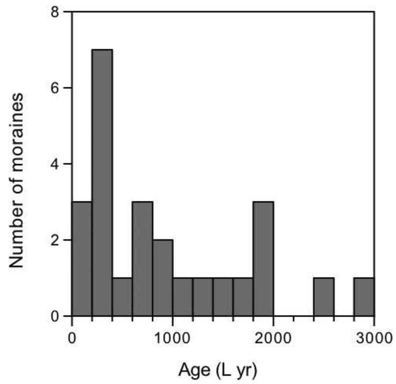

FIGURE 6. Frequency histogram showing the lichenometric age distribution of moraines in the Sagavanirktok River valley and Oolah Valley. The most recent periods of moraine stabilization occurred around 700 and 300 L yr (A.D. 1250 and 1650).

Arrigetch Peaks, to 1710 ± 110 m near Atigun Pass, to 1980 ± 100 m near Mount Michelson (Fig. 7). The uncertainties are the standard deviations within each region and reflect the important influence of snow drift, shading, and other microclimate and minor debris-cover effects on the ELA (Lie et al., 2003). For comparison, ELAs reconstructed by Ellis and Calkin (1984) increase from 1340 ± 40 m in the Arrigetch Peaks to 1755 ± 70 m in Atigun Pass. Their values are based on a smaller subsample of glaciers, a higher AAR (0.67), and reconstructions of the maximum Neoglacial ice margins, which lie beyond the LIA moraines for some glaciers.

"MODERN" ELAs AND ΔELA

On the basis of glacier extents photographed in 1955 and 1970, and using an AAR of 0.48, the average ELA of the 114 study glaciers increases from 1470 ± 100 m in the Arrigetch Peaks, to 1730 ± 110 m near Atigun Pass, to 2001 ± 95 m near Mount Michelson (Appendix; Fig. 7). These values are consistent with those based on a larger data set of 940 glaciers across the Brooks Range recently mapped by Balascio et al. (2005). Our first-order trend in ELA bisects the third-order trend surface calculated by Balascio et al. (2005) to interpolate the "modern" ELA surface across the Brooks Range. They used an AAR of 0.58, which results in ELA estimates that are a few tens of meters lower compared to our AAR value of 0.48. Their study focused on ELA lowering during the late Wisconsin for which the position of "modern" ELA is secondary. A least-squares linear regression fit to our ELA data shows a gradient of 1.2 m km^{-1} ($R^2 = 0.71$; $p < 0.01$) for an east-west transect along the range crest (Fig. 7). This ELA gradient is also consistent with the glaciation thresholds for Brooks Range glaciers shown by Porter et al. (1983).

Our ELA estimates for "modern" glaciers differ from previous measurements, probably due to differences in the reference period. Between 1976 and 1979, ELAs measured on three glaciers in the central Brooks Range (Ellis and Calkin, 1982; Calkin et al., 1985) were about 120 m higher than the average "modern" ELA of 60 glaciers near Atigun Pass calculated in this study. In 1975, a pronounced increase in summer temperature occurred in Alaska (Kelly et al., 1982; Serreze et al., 2000). The modern glacier positions that we used were reached by 1970 as inferred from aerial photographs and U.S. Geological Survey topographic maps, prior to the abrupt warming of the mid 1970s. The glaciers instrumented for mass-balance studies between 1977 and 1981 (Ellis and Calkin, 1982, 1984) were probably readjusting to the warmer summer temperature. ELAs rose 100 m above the glaciers in the summer of 1977 and remained at the head of the glaciers during the summers of 1978 and 1979 (Ellis and Calkin, 1982). Thus, our estimates most likely represent an average over several years, whereas the direct measurements in the late 1970s captured the inter-annual variability.

The difference between the ELAs of "modern" and LIA glaciers (ΔELA) shows that ELAs of the 114 study glaciers were lower by an average of 51 ± 29 m during the LIA maximum (Table 1; Appendix). This value assumes an AAR of 0.58 for LIA glaciers and 0.48 for "modern" glaciers. If instead the AARs for the "modern" and LIA glaciers were equal, then the estimated ΔELA would decrease to 26 m, and this value is relatively insensitive to actual AAR, assuming only that the AAR was the same for modern and LIA. Conversely, if the AAR values differed by 0.2 ("modern" AAR = 0.38), for example, then the ΔELA would increase by 27 m (to 78 m). Our ΔELA estimate is probably a maximum value because the elevations inferred for the reconstructed LIA glaciers were based on the "modern" glacier topography. Because the surfaces of the glaciers were higher during the LIA, our ELA estimates for the LIA underestimate the true altitude, and therefore the ΔELA values are probably too large.

Linear-regression analysis (Fig. 7) shows essentially parallel trends in ELA for both "modern" and LIA ELAs (i.e., ΔELA was uniform across the Brooks Range), suggesting generally similar climatic conditions and moisture flow paths during the LIA maximum and "modern." This is true for both the northeastern sector of the range, which is more strongly influenced by its proximity to the Arctic Ocean, and for the central Brooks Range, where Pacific-derived storms dominate (see discussion below).

Discussion

LITTLE ICE AGE CLIMATE INFERRED FROM ΔELA VALUES

The average ΔELA of 51 ± 29 m for LIA maximum glaciers in the Brooks Range is considerably less than for many other high-latitude regions. For example, ΔELA estimates between 100 and 400 m have been reported for the LIA in western Norway (e.g., Dahl and Nesje, 1992), Baffin Island, Canada (Locke and Locke, 1977), and Iceland (Mackintosh et al., 2002). Spatial variability in climate change might explain the range of LIA ΔELA estimates for these regions. Differences in the reference period used to calculate "modern" glacier ELAs might also help to explain the discrepancy. Regardless, the ΔELA (51 m) determined in this study is unexpectedly small relative to most previously reported estimates, and suggests either that summer temperature did not lower as much as in other regions, or that a paucity of cold-season accumulation limited the growth of LIA glaciers in the Brooks Range.

The temperature difference associated with an ELA shift of 51 m can be inferred if we assume that changes in ELA are controlled only by temperature and by applying an environmental lapse rate. Recent measurements on McCall Glacier (Matt Nolan, unpublished data; Klok et al., 2006) indicate that the mean annual lapse rate on the glacier surface matches the expected free-air adiabatic lapse rate of 6 °C km^{-1}, but that the average summer lapse rate is only 2 °C km^{-1}; on time scales of hours to days the rate can vary widely and include negative values. Rabus and Echelmeyer (1998) measured a lapse rate at the glacier of around 6 °C km^{-1} using ice temperatures at 10 m depth as a proxy for mean annual air temperature. This gradient has remained

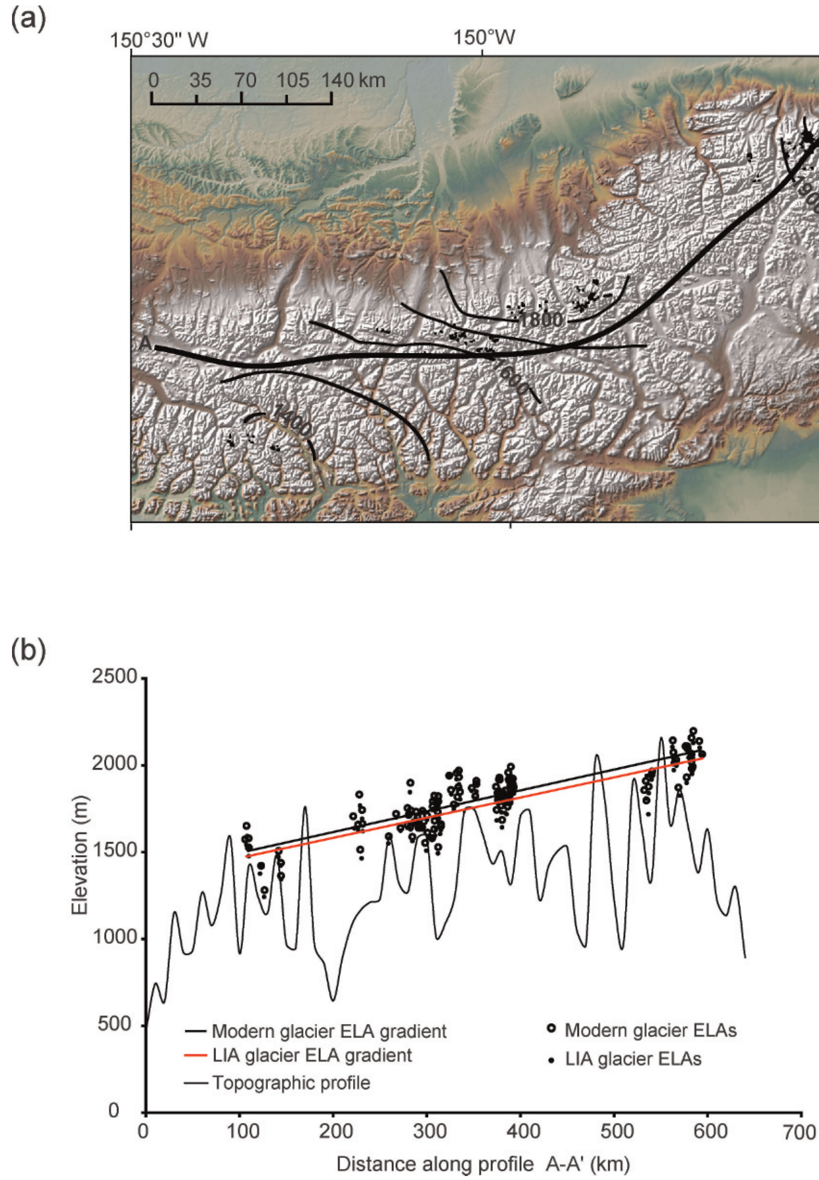

FIGURE 7. (a) Contoured Little Ice Age (LIA) equilibrium-line altitudes (ELAs) of 114 glaciers (black shapes). Paleo-ELAs rise from southwest to northeast across the range. Contour interval is 100 m. (b) Topographic profile from A to A′ across the crest of the Brooks Range shown in (a) with the ELAs of 114 "modern" and LIA glaciers. Lines are least-squares linear regressions. "Modern" and LIA ELAs rise eastward across the range at 1.2 m km^{-1} (R^2 = 0.71, $p > 0.01$).

consistent since 1972 when similar measurements were made (Rabus and Echelmeyer, 2002). Other evidence suggests that lapse rates in the central Brooks Range are higher: (1) summer temperatures measured between 1975 and 1978 at four Haul Road climate stations (Haugen, 1979) show a lapse rate of 9 °C km^{-1}, and (2) short-term weather data from the Grizzly Glacier show a lapse rate of 12 °C km^{-1} (Calkin et al., 1985).

To estimate the temperature decrease associated with an average ELA lowering of 51 m during the LIA maximum, we assume that the ELA is controlled by ablation-season temperature only and apply the range of measured local environmental lapse rates in the Brook Range (2–12 °C km^{-1}). This approach suggests a temperature reduction of between 0.1 and 0.6 °C (e.g., 2 °C km^{-1} × 51 m = 0.1 °C).

This range of temperature lowering is less than has been inferred based on tree-ring and other paleoclimate evidence. The proxy climate record closest to the Brooks Range is based on a white spruce (*Picea glauca*) tree-ring series from across northern Alaska, south of the Brooks Range (Jacoby et al., 1999; recently reinterpreted and expanded by D'Arrigo et al., 2006). The record spans the last 300 yr and indicates that summer temperatures during the coldest two-decade interval, centered on A.D. 1690, were about 0.8 °C lower than during the reference period of A.D. 1960–1970; similar cooling took place around A.D. 1830. More pronounced cooling of between 1.3 and 2.0 °C has been inferred for the LIA in central Alaska (Hu et al., 2001; Clegg et al., 2005). Taken together, these values are consistent with the 1.0 to 1.5 °C LIA cooling estimated for elsewhere in the Arctic (e.g., Bradley and Jones, 1993).

Considering the widespread evidence for LIA warm-season temperature reduction of about 1 °C at northern high latitudes, we expect glaciers to have responded commensurately. If temperature was the only variable controlling mass balance, and assuming an environmental lapse rate of 6 °C km^{-1}, then a 1 °C temperature reduction implies a ΔELA of about 170 m (i.e., 6 °C^{-1} km × 1 °C), or about three times more than determined in this study. To reconcile this discrepancy, and assuming that our ΔELA values are robust, then some other variable must have inhibited the expansion of LIA glaciers in the Brooks Range. A decrease in cold-season precipitation is one explanation, although we cannot rule out the possibility that factors related to radiation, including cloud cover, also influenced the mass balance.

The various combinations of accumulation-season precipitation and ablation-season temperature at the ELA of glaciers have been investigated using several approaches. These include mass/energy-balance modeling (e.g., Oerlemans and Fortuin, 1992), and empirical relations derived from climate data at the ELA of instrumented glaciers (e.g., Ohmura et al., 1992), among others. As discussed by Seltzer (1994), these approaches converge on the conclusion that a 1 °C change in mean ablation-season temperature is accommodated by a change in mean annual accumulation of about 300 mm at the ELA of glaciers from a range of climates. At polar latitudes, however, where precipitation receipts are low, a 1 °C temperature change is offset by a smaller change in precipitation, that is, the relation between temperature and accumulation at the ELA is exponential (Leonard, 1989; Miller and de Vernal, 1992; Lie et al., 2003; Braithwaite et al., 2006). Quantifying the extent to which the high elevations of the Brooks Range were drier than present during the LIA is difficult because the relation between these variables is not well constrained for Brooks Range glaciers. Furthermore, little is known about the present-day distribution of precipitation in the range to compare with LIA estimates.

We suggest that cold-season accumulation in the Brooks Range was reduced during the LIA. In contrast, other proxy climate records from lower elevations in northern Alaska (Hu et al., 2001; Mann et al., 2002b; Clegg et al., 2005) indicate increased moisture during this period. Possible explanations for this difference are a seasonal bias in the proxy climate records, or the difference in the measure of precipitation being estimated (effective versus absolute moisture). The difference might also reflect the spatial heterogeneity in precipitation patterns that are expected across Beringia as atmospheric circulation patterns shifted (e.g., Edwards et al., 2001).

ATMOSPHERIC CIRCULATION DURING THE LITTLE ICE AGE

The climate of the Brooks Range is spatially variable. The range forms a physical border between Alaska's continental climate regime to the south and arctic climate to the north. South-to-southwesterly winds bring moisture from the north Pacific inland, and are responsible for high snowfall years in the instrumental record north of the Brooks Range, where shifts in zonal flow significantly impact annual precipitation (Stone et al., 2002). L'Heureux et al. (2004), however, inferred that anomalous southerly flow may lead to drying of the region through a rain shadow effect. Moisture availability in the Brooks Range might also be affected by changes in atmospheric circulation related to the Arctic Oscillation (AO) (Serreze et al., 2000). In the negative-index mode of the AO, positive surface pressures over the Arctic Ocean drive the anti-cyclonic Beaufort Gyre. As suggested by Stone et al. (2002), high atmospheric pressure over northern Alaska tends to increase northerly flow that reduces precipitation along the North Slope by blocking inland flow of moisture-bearing winds from the North Pacific. Recent studies (e.g., Stone et al., 2002; L'Heureux et al., 2004) highlight the importance of the AO on moisture distribution in the Arctic, but have found no significant correlation between the AO index and precipitation along the North Slope in northern Alaska.

The boundary between the cold surface air over the Arctic Ocean and warmer air to the south determines the position of the Arctic front, which oscillates with the seasons (Serreze et al., 2001), and influences the moisture distribution in the northern Brooks Range (Rabus and Echelmeyer, 1998). The front is well developed in northern Alaska during summer where it coincides with the northern flank of the Brooks Range and the zone of maximum precipitation. The relation between temperature and precipitation in northern Alaska is not simple, however. Curtis et al. (1998) suggested that decreased cloud cover (and thus decreased storm frequency) is often associated with warmer temperatures, which might explain why recent warming in northern Alaska has coincided with decreased annual precipitation, while annual precipitation has increased over most of the Arctic during the 20th century (Serreze et al., 2000). Nonetheless, the cold air north of the Arctic front is drier than to the south, and the southward displacement of the Arctic front would therefore coincide with the advection of cooler and drier air masses southward into the Brooks Range.

Conclusion

This study provides new glacial-geologic evidence suggesting that precipitation did not increase, and most liked decreased in the Brooks Range as glaciers attained their maximum LIA positions. Our reconstructions indicate that glacier expansion during the LIA was relatively minor compared with LIA advances of other high-latitude mountains, with an ELA lowering of only about 51 ± 29 m. Previously published proxy climate records from central and northern Alaska indicate that warm-season temperatures were about 1 °C lower during the Little Ice Age, which should have lead to an ELA lowering of about 170 m, assuming that temperature change was the only control on ELA. This did not occur, and we therefore hypothesize that glacier expansion was suppressed because precipitation decreased. We suggest that a prolonged southward shift of the Arctic front over the Brooks Range could have resulted in a reduction in accumulation on the glaciers. This finding provides an alternative perspective to previous paleoclimate reconstructions elsewhere in Alaska, which indicate increased moisture during the LIA, and suggests that more research is required to resolve this apparent discrepancy.

Acknowledgments

Nicholas Balascio assisted in the field and helped with data processing. Gordon Jacoby provided temperature reconstructions from northern Alaska tree-ring data. We thank the anonymous reviewers of earlier versions for their constructive input. This study was funded by NSF grants (OPP-9977972 and OPP-9977974), and graduate student grants from Geological Society of America and Sigma Xi.

References Cited

Balascio, N. L., Kaufman, D. S., and Manley, W. F., 2005: Equilibrium-line altitudes during the last glacial maximum across the Brooks Range, Alaska. *Journal of Quaternary Science*, 20: 821–838.

Benn, D. I., Lewis, A. O., Osmaston, H. A., Seltzer, G. O., Porter, S. C., and Mark, B., 2005: Reconstruction of equilibrium-line altitudes for tropical and sub-tropical glaciers. *Quaternary International*, 138-139: 8–21.

Bradley, R. S., and Jones, P. D., 1993: 'Little Ice Age' summer temperature variations: their nature and relevance to recent global warming trends. *The Holocene*, 3: 367–376.

Braithwaite, R. J., Raper, S. C. B., and Chutko, K., 2006: Accumulation at the equilibrium-line altitude of glaciers inferred from a degree-day model and tested against field observations. *Annals of Glaciology*, 43: 329–334.

Calkin, P. E., and Ellis, J. M., 1980: A lichenometric dating curve and its application to Holocene glacier studies in the central Brooks Range, Alaska. *Arctic and Alpine Research*, 12: 245–264.

Calkin, P. E., Ellis, J. M., Haworth, L. A., and Burns, P. E., 1985: Cirque glacier regime and Neoglaciation, Brooks Range, Alaska. *Zeitschrift fur Gletscherkunde und Glazialgeologie*, 21: 371–378.

Clegg, B. F., Tinner, W., Henderson, A., Bigler, C., and Hu, F. S., 2005: Spatial manifestation of the Little Ice Age in Alaska. *EOS Transactions of the American Geophysical Union*, 86(52): abstract PP31A-1513.

Curtis, J., Wendler, G., Stone, R., and Dutton, E., 1998: Precipitation decrease in the western Arctic with special emphasis on Barrow and Barter Island, Alaska. *International Journal of Climatology*, 18: 1687–1707.

D'Arrigo, R., Wilson, R., and Jacoby, G., 2006: On the long-term context of late 20th century warming. *Journal of Geophysical Research*, 111: D03103, doi: 10.1029/2005JD006352.

Dahl, S. O., and Nesje, A., 1992: Paleoclimate implications based on the equilibrium-line altitude depressions of reconstructed Younger Dryas and Holocene cirque glaciers in inner Nordfjord, western Norway. *Palaeogeography, Palaeoclimatology, and Palaeoecology*, 94: 87–97.

Dahl, S. O., and Nesje, A., 1996: A new approach of calculating Holocene winter precipitation by combining glacier equilibrium-line altitudes and pine-tree limits; a case study from Hardangerjøkulen, central southern Norway. *The Holocene*, 6: 381–398.

Detterman, R. L., Bowsher, A. L., and Dutro, T., 1958: Glaciation on the Arctic Slope of the Brooks Range, northern Alaska: *Arctic*, 11: 43–61.

Dyurgerov, M., 2002: Glacier mass balance and regime: data of measurements and analysis. Boulder: University of Colorado, INSTAAR Occasional Paper no. 55.

Edwards, M. E., Mock, C. J., Finney, B. P., Barber, V. A., and Bartlein, J., 2001: Potential analogues for paleoclimatic variations in eastern interior Alaska during the past 14,000 yr: atmospheric-circulation controls of regional temperature and moisture responses. *Quaternary Science Reviews*, 20: 189–202.

Ellis, J. M., and Calkin, P. E., 1979: Nature and distribution of glaciers, neoglacial moraines, and rock glaciers, east-central Brooks Range, Alaska. *Arctic and Alpine Research*, 11: 403–420.

Ellis, J. M., and Calkin, P. E., 1982: 1977–1981: an interval of descending ELA's and cooling temperatures, central Brooks Range, Alaska. *Geological Society of America Programs with Abstracts*, 14(7): 483.

Ellis, J. M., and Calkin, P. E., 1984: Chronology of Holocene glaciation, central Brooks Range, Alaska. *Geological Society of America Bulletin*, 95: 897–912.

Ellis, J. M., Hamilton, T. D., and Calkin, P. E., 1981: Holocene glaciation of the Arrigetch Peaks, Brooks Range, Alaska. *Arctic*, 34: 158–168.

Evison, L. H., Calkin, P. E., and Ellis, J. M., 1996: Late-Holocene glaciation and twentieth-century retreat, northeastern Brooks Range, Alaska. *The Holocene*, 6: 17–24.

Hamilton, T. D., 1979: Surficial geologic map of Chandler Lake Quadrangle, Alaska. U.S. Geological Survey Miscellaneous Field Studies Map MF-1121, scale 1: 250,000.

Hamilton, T. D., 1981: Surficial geologic map of Survey Pass Quadrangle, Alaska. U.S. Geological Survey Miscellaneous Field Studies Map MF-1320, scale 1: 250,000.

Hamilton, T. D., 1986: Late Cenozoic glaciation of the central Brooks Range. *In* Hamilton, T. D., Reed, K. M., and Thorson, R. M. (eds.), *Glaciation in Alaska—The geologic record* Alaska Geological Society, 9–49.

Haugen, R. K., 1979: Climatic investigation along the Yukon River to Prudhoe Bay Haul Road, Alaska, 1975–78. Informal etract from final Federal Highway Administration Contract Report, Environmental investigations along the Yukon River to Prudhoe Bay Haul Road, Alaska. U.S. Army Corps of Engineers Cold Regions Research and Engineering Laboratory: Hanover, New Hampshire.

Hu, F. S., Ito, E., Brown, T. A., Curry, B. B., and Engstrom, D. R., 2001: Pronounced climatic variation in Alaska during the last two millennia. *Proceedings of the National Academy of Sciences*, 98: 10552–10556.

Innes, J. L., 1985: Lichenometry. *Progress in Physical Geography*, 9: 187–254.

Jacoby, G. C., Workman, K. W., and D'Arrigo, R. D., 1999: Laki eruption of 1783, tree rings, and disaster for northwest Alaska Inuit. *Quaternary Science Reviews*, 18: 1365–1371.

Kelly, P. M., Jones, P. D., Sear, C. B., Cherry, B. S. G., and Tavakol, R. K., 1982: Variations in surface air temperatures: Part 2. Arctic regions, 1881–1980. *Monthly Weather Review*, 110: 71–83.

Klok, L., Nolan, M., and van den Drocke, M., 2006: Analysis of meteorological data and the surface energy balance of McCall Glacier, Alaska. *Journal of Glaciology*, 51: 451–461.

L'Heureux, M. L., Mann, M. E., Cook, B. I., Gleason, B. E., and Vose, R. S., 2004: Atmospheric circulation influences on seasonal precipitation patterns in Alaska during the latter 20th century. *Journal of Geophysical Research*, 109: D06106, doi: 10.1029/2003JD003845.

Leffingwell, E. deK., 1919: The Canning River region, northeastern Alaska. *U.S. Geological Survey Professional Paper*, 109.

Leonard, E. M., 1989: Climate change in Colorado Rocky Mountains: estimates based on modern climate at late Pleistocene equilibrium lines. *Arctic and Alpine Research*, 21: 245–255.

Lie, Ø., Dahl, S. O., and Nesje, A., 2003: Theoretical equilibrium-line altitudes and glacier buildup sensitivity in southern Norway based on meteorological data in a geographical information system. *The Holocene*, 13: 373–380.

Locke, C. W., and Locke, W. W., 1977: Little ice age snow-cover extent and paleoglaciation thresholds: north-central Baffin Island, NWT, Canada. *Arctic and Alpine Research*, 9: 291–300.

Lowell, T. V., 2000: As climate changes, so do glaciers. *Proceedings of National Academy of Sciences*, 97: 1351–1354.

Luckman, B. H., and Wilson, R. J. H., 2005: Summer temperatures in the Canadian Rockies during the last millennium; a revised record. *Climate Dynamics*, 24: 131–144.

Mackintosh, A. N., Dugmore, A. J., and Hubbard, A. L., 2002: Holocene climatic changes in Iceland: evidence for modeling glacier length fluctuations at Sólheimajökull. *Quaternary International*, 91: 39–52.

Mann, D. H., Peteet, D. M., Reanier, R. E., and Kunz, M. L., 2002a: Responses of an Arctic landscape to late glacial and early Holocene climatic changes: the importance of moisture. *Quaternary Science Reviews*, 21: 997–1021.

Mann, D. H., Heiser, P. A., and Finney, B. P., 2002b: Holocene history of the great Kobuk sand dunes, northwestern Alaska. *Quaternary Science Reviews*, 21: 709–731.

Miller, G. H., and de Vernal, A., 1992: Will greenhouse warming lead to northern hemisphere ice-sheet growth? *Nature*, 355: 244–246.

Moberg, A., Sonechkin, D. M., Holmgren, K., Datsenko, N. M., and Karlén, W., 2005: Highly variable northern hemisphere temperatures reconstructed from low- and high-resolution proxy data. *Nature*, 433: 613–617.

Nesje, A., and Dahl, S. O., 2003: The 'Little Ice Age'—Only temperature? *The Holocene*, 13: 139–145.

Oerlemans, J., 2005: Extracting a climate signal from 169 glacier records. Sciencexpress: doi: 10.1126/science.1107046.

Oerlemans, J., and Fortuin, J. P. F., 1992: Sensitivity of glaciers and small ice caps to greenhouse warming. *Science*, 258(5079): 115–117.

Ohmura, A., Kasser, P., and Funk, M., 1992: Climate at the equilibrium line of glaciers. *Journal of Glaciology*, 6: 391–398.

Orvig, S., 1961: McCall Glacier, Alaska: meteorological observations 1957–1958. *Arctic Institute of North America Paper*, 8.

Overpeck, J., Hughen, K., Hardy, D., Bradley, R., Case, R., Douglas, M., Finney, B., Gajewski, K., Jacoby, G., Jennings, A., Lamoureux, S., Lasca, G., MacDonals, G., Moore, J., Retelle, M., Smith, S., Wolfe, A., and Zielinski, G., 1997: Arctic environmental changes of the last four centuries. *Science*, 278: 1251–1256.

Polissar, P. J., Abbottt, M. B., Wolfe, A. P., Bezada, M., Rull, V., and Bradley, R. S., 2006: Solar modulation of Little Ice Age climate in the tropical Andes. *Proceedings of the National Academy of Sciences*, 103: 8937–8942.

Porter, S. C., and Denton, G. H., 1967: Chronology of Neoglaciation in the North American Cordillera. *American Journal of Science*, 265: 177–210.

Porter, S. C., Pierce, K. L., and Hamilton, T. D., 1983: Late Wisconsin mountain glaciation in the western United States. *In* Porter, S. C. (ed.), *Late Quaternary Environments of the United States*. Minneapolis, Minnesota: University of Minnesota Press, 71–111.

Rabus, B. T., and Echelmeyer, K. A., 1998: The mass balance of McCall Glacier, Brooks Range, Alaska, U.S.A.; its regional relevance and implications for climate change in the Arctic. *Journal of Glaciology*, 44: 333–351.

Rabus, B. T., and Echelmeyer, K. A., 2002: Increase of 10 m ice temperature: climate warming or glacier thinning? *Journal of Glaciology*, 48: 279–286.

Seltzer, G. O., 1994: Climatic interpretation of alpine snowline variations on millennial time scales. *Quaternary Research*, 41: 154–159.

Serreze, M. C., and Hurst, C. M., 2000: Representation of mean arctic precipitation from NCEP-NCAR and ERA reanalyses. *Journal of Climate*, 13: 182–201.

Serreze, M. C., Walsh, J. E., Chapin, F. S., Osterkamp, T., Dyurgerov, M., Romanovsky, V., Oechel, W. C., Morison, J., Zhang, T., and Barry, R., 2000: Observational evidence of recent change in the northern high-latitude environment. *Climate Change*, 46: 159–207.

Serreze, M. C., Lynch, A. H., and Clark, M. P., 2001: The arctic frontal zone as seen in the NCEP-NCAR reanalysis. *Journal of Climate*, 14: 1550–1567.

Sikorski, J., 2004: Winter accumulation at the equilibrium line of Little Ice Age glaciers. M.S. thesis. Northern Arizona University: Flagstaff, 118 pp.

Solomina, O., and Calkin, P. E., 2003: Lichenometry as applied to moraines in Alaska, U.S.A., and Kamchatka, Russia. *Arctic, Antarctic, and Alpine Research*, 35: 129–143.

Stone, R. S., Dutton, E. G., Harris, J. M., and Longenecker, D., 2002: Earlier spring snowmelt in northern Alaska as an indicator of climate change. *Journal of Geophysical Research*, 107: doi: 10.1029/2000JD000286.

U.S. Geological Survey, 1998: Standards for digital line graphs. National Mapping Program Technical Instructions, version 07/98.

Wiles, G. C., D'Arrigo, R. D., Villalba, R., Calkin, P. E., and Barclay, D. J., 2004: Century-scale solar variability and Alaskan temperature change over the past millennium. *Geophysical Research Letters*, 31: L15203, doi: 10.1029/2004GL020050.

MS accepted June 2008

APPENDIX

Coordinates, physical parameters, and equilibrium-line altitudes (ELAs) for both extant and LIA glaciers in the Brooks Range, Alaska. Listed from west to east.

		Modern									Little Ice Age									
Longitude (°W)	Latitude (°N)	Minimum elevation (m)	Maximum elevation (m)	Length (km)	Perimeter (km)	Area (km^2)	Compact-ness[a]	Aspect from (0°)	Slope (degree)	ELA (m)	Minimum elevation (m)	Maximum elevation (m)	Length (km)	Perimeter (km)	Area (km^2)	Compact-ness[a]	Aspect from (0°)	Slope (degree)	ELA (m)	ΔELA (m)
154.967	67.436	1365	1879	2.00	6.72	1.12	0.31	324	13	1574	1338	1880	2.00	7.20	1.30	0.31	316	13	1541	33
154.956	67.469	1477	1965	1.60	5.16	0.74	0.35	5	13	1656	1424	1966	2.20	6.48	0.94	0.28	11	11	1592	64
154.929	67.417	1286	1825	2.10	13.44	1.92	0.13	25	14	1575	1216	1824	2.70	15.36	2.28	0.12	30	12	1531	44
154.909	67.408	1237	1871	1.90	8.52	0.91	0.16	52	17	1549	1226	1871	1.90	8.88	0.98	0.16	52	16	1477	72
154.634	67.481	1298	1548	0.90	3.48	0.41	0.43	21	13	1421	1244	1548	1.30	4.08	0.57	0.43	26	12	1376	45
154.605	67.443	1375	1486	0.40	1.80	0.13	0.50	6	13	1432	1362	1500	0.50	2.28	0.21	0.50	15	11	1419	13
154.532	67.472	1148	1500	1.00	4.08	0.37	0.28	349	14	1272	1125	1500	1.10	4.56	0.45	0.27	355	14	1242	30
154.169	67.392	1219	1729	1.80	6.72	1.16	0.32	358	15	1495	1208	1729	1.90	7.80	1.38	0.28	356	15	1472	23
154.111	67.377	1316	1576	0.50	2.40	0.17	0.37	9	16	1440	1285	1604	0.80	3.12	0.23	0.30	356	16	1423	17
154.108	67.406	1257	1452	0.50	2.16	0.17	0.47	19	18	1362	1248	1453	0.60	2.28	0.20	0.48	23	16	1343	19
152.257	68.211	1562	1826	0.90	3.12	0.36	0.46	14	13	1708	1514	1827	1.30	3.96	0.50	0.40	18	11	1637	71
152.158	68.204	1504	1817	1.20	6.36	1.01	0.31	333	16	1685	1467	1818	1.70	7.44	1.33	0.30	332	12	1627	58
152.108	68.197	1706	1877	0.50	1.68	0.14	0.63	345	21	1821	1626	1878	0.50	2.16	0.22	0.60	346	19	1767	54
152.072	68.196	1368	1695	0.90	3.00	0.34	0.48	353	15	1516	1359	1695	1.10	3.84	0.46	0.39	0	12	1464	52
152.057	68.192	1575	1884	0.70	2.52	0.27	0.54	358	20	1752	1546	1884	0.90	2.88	0.34	0.51	353	17	1692	60
151.389	68.041	1421	1739	1.00	3.36	0.32	0.35	358	14	1603	1374	1740	1.20	3.72	0.35	0.32	358	14	1550	53
151.181	68.172	1614	1827	0.70	2.88	0.32	0.49	26	15	1739	1548	1828	1.10	3.72	0.44	0.40	19	14	1700	39
151.067	68.183	1476	1922	1.40	5.16	0.85	0.40	334	17	1665	1422	1923	1.40	5.52	0.99	0.41	336	16	1624	41
150.889	68.133	1531	1804	0.70	3.12	0.30	0.38	310	21	1674	1441	1804	0.90	3.84	0.35	0.30	312	20	1639	35
150.888	68.145	1582	2042	1.70	6.12	0.80	0.27	345	13	1802	1563	2042	2.00	6.12	0.88	0.29	343	12	1724	78
150.859	68.142	1426	2030	2.40	10.20	1.90	0.23	13	10	1762	1410	2030	2.60	10.56	1.98	0.22	12	10	1706	56
150.821	68.223	1757	2025	1.10	4.56	0.64	0.39	18	15	1903	1703	2025	1.10	5.16	0.92	0.43	21	13	1845	58
150.813	68.138	1476	1951	2.20	9.12	1.20	0.18	5	10	1673	1432	1951	2.20	9.12	1.47	0.22	7	9	1631	42
150.805	68.166	1587	1969	1.40	5.04	0.52	0.26	5	12	1754	1521	1969	1.60	5.52	0.63	0.26	11	11	1725	29
150.769	68.118	1396	1721	1.60	5.88	0.98	0.36	1	8	1596	1386	1721	1.70	6.12	1.09	0.36	357	8	1564	32
150.717	68.145	1455	2110	1.40	6.96	0.68	0.18	330	14	1695	1399	2110	1.50	7.32	0.76	0.18	329	14	1660	35
150.669	68.152	1488	1929	1.90	14.52	2.04	0.12	9	9	1758	1380	1929	1.90	14.88	2.35	0.13	11	9	1693	65
150.643	68.169	1564	1723	0.40	2.28	0.19	0.45	347	20	1684	1463	1727	0.60	2.76	0.25	0.41	342	18	1654	30
150.631	68.142	1555	1868	1.00	3.96	0.44	0.35	345	16	1729	1532	1868	1.10	4.44	0.50	0.32	341	15	1677	52
150.627	68.096	1578	1765	0.90	3.72	0.42	0.38	17	8	1680	1553	1765	1.00	3.96	0.50	0.40	33	8	1670	10
150.610	68.087	1577	1700	0.50	1.92	0.18	0.60	12	11	1647	1560	1700	0.70	2.16	0.21	0.55	10	10	1634	13
150.526	68.104	1563	1683	0.40	1.56	0.10	0.52	354	19	1650	1556	1683	0.50	1.80	0.13	0.52	342	20	1636	14
150.512	68.103	1669	1782	0.40	1.32	0.08	0.60	13	15	1747	1658	1782	0.40	1.44	0.10	0.59	18	14	1729	18
150.474	68.110	1535	1807	0.60	2.64	0.20	0.36	8	24	1692	1467	1813	0.80	3.12	0.28	0.36	12	21	1644	48
150.420	68.041	1441	1796	1.20	4.68	0.48	0.28	3	13	1553	1402	1796	1.60	7.92	0.87	0.18	3	12	1509	44
150.401	68.033	1644	1911	0.70	4.32	0.29	0.19	54	18	1733	1547	1911	1.00	5.28	0.51	0.23	48	13	1688	45
150.372	68.047	1546	1730	0.70	2.52	0.22	0.44	20	10	1614	1487	1732	1.10	3.24	0.31	0.37	25	9	1583	31
150.257	68.046	1618	1936	1.10	3.72	0.47	0.43	24	14	1787	1607	1937	1.20	4.20	0.51	0.37	25	14	1742	45
150.231	68.031	1677	1866	0.70	2.76	0.30	0.49	77	11	1794	1642	1867	0.90	3.24	0.37	0.44	86	11	1752	42
150.192	68.037	1521	1772	0.80	2.88	0.28	0.43	8	15	1639	1442	1773	1.00	3.48	0.39	0.40	11	13	1596	43
150.172	68.036	1507	1957	1.20	6.00	0.64	0.22	35	14	1686	1442	2015	1.30	4.92	0.75	0.39	353	14	1635	51

APPENDIX
Continued.

		Modern									Little Ice Age									
Longitude (°W)	Latitude (°N)	Minimum elevation (m)	Maximum elevation (m)	Length (km)	Perimeter (km)	Area (km^2)	Compact-ness[a]	Aspect from (0°)	Slope (degree)	ELA (m)	Minimum elevation (m)	Maximum elevation (m)	Length (km)	Perimeter (km)	Area (km^2)	Compact-ness[a]	Aspect from (0°)	Slope (degree)	ELA (m)	ΔELA (m)
150.167	68.123	1642	2014	1.00	4.68	0.63	0.36	353	14	1824	1620	1957	2.10	7.08	0.89	0.22	32	11	1790	34
150.138	68.123	1690	2009	1.20	4.56	0.59	0.36	10	11	1788	1528	2010	1.60	5.64	0.95	0.38	354	10	1747	41
150.123	68.025	1466	1757	1.20	4.08	0.36	0.27	348	15	1530	1396	1757	1.20	5.16	0.58	0.27	355	11	1493	37
150.120	68.104	1645	1951	0.90	3.60	0.48	0.46	359	14	1823	1619	1951	1.00	3.84	0.55	0.47	6	13	1797	26
150.100	68.126	1647	1856	0.90	2.76	0.20	0.33	56	15	1785	1596	1856	0.90	3.12	0.27	0.35	49	16	1768	17
150.088	68.095	1598	1889	1.40	6.12	0.85	0.29	331	10	1734	1475	1889	1.40	7.80	1.04	0.21	339	9	1694	40
150.055	68.103	1529	1712	0.80	3.12	0.30	0.38	343	10	1645	1474	1712	1.10	3.84	0.42	0.36	327	9	1605	40
150.033	68.100	1578	1744	0.70	2.88	0.24	0.37	355	10	1657	1542	1744	1.10	3.72	0.41	0.37	9	9	1628	29
149.791	68.331	1733	2150	1.50	7.68	1.57	0.33	13	14	1964	1725	2150	1.50	7.68	1.69	0.36	13	14	1935	29
149.739	68.288	1702	2012	0.80	3.24	0.42	0.50	15	12	1858	1690	2011	0.90	3.48	0.45	0.47	15	12	1833	25
149.682	68.254	1636	1834	0.80	2.88	0.25	0.38	356	11	1769	1607	1835	0.80	3.24	0.31	0.37	0	10	1746	23
149.601	68.322	1754	2145	0.90	3.72	0.42	0.39	335	18	2000	1705	2167	1.10	4.08	0.55	0.42	330	16	1920	80
149.583	68.284	1584	1983	0.90	4.20	0.41	0.29	0	18	1829	1557	1983	1.00	4.44	0.49	0.31	1	17	1774	55
149.558	68.281	1767	1946	0.40	1.80	0.14	0.53	28	19	1889	1720	1947	0.50	1.92	0.16	0.55	28	18	1862	27
149.549	68.297	1736	2130	1.00	3.48	0.44	0.46	33	17	1998	1702	2130	1.00	3.96	0.50	0.40	39	17	1949	49
149.536	68.342	1663	2233	2.30	6.48	1.13	0.34	23	12	1972	1570	2233	2.50	7.92	1.36	0.27	18	11	1890	82
149.507	68.335	1673	2031	1.10	5.28	0.80	0.36	6	14	1847	1614	2032	1.50	6.36	0.93	0.29	4	12	1803	44
149.204	68.323	1759	1983	1.00	3.12	0.33	0.42	2	16	1884	1665	1983	1.10	3.72	0.39	0.35	8	16	1853	31
149.116	68.284	1677	1990	1.00	3.48	0.44	0.46	335	15	1848	1609	1990	1.00	3.96	0.49	0.40	333	14	1808	40
149.095	68.288	1727	2055	1.00	3.72	0.48	0.44	335	16	1945	1692	2055	1.10	3.96	0.51	0.41	335	16	1897	48
149.084	68.351	1700	2104	1.10	6.48	0.78	0.23	18	14	1914	1603	2104	1.10	8.04	0.98	0.19	12	14	1849	65
148.583	68.329	1703	2096	0.90	3.12	0.41	0.53	15	17	1888	1610	2096	0.90	3.96	0.50	0.40	4	16	1841	47
148.562	68.290	1647	1773	0.40	1.56	0.11	0.56	0	18	1735	1606	1775	0.60	2.16	0.19	0.51	11	12	1682	53
148.527	68.291	1669	1965	0.70	2.40	0.22	0.49	345	21	1827	1642	1965	0.90	2.76	0.26	0.43	344	19	1780	47
148.510	68.296	1665	2032	0.90	3.60	0.35	0.34	341	15	1870	1544	2032	1.10	4.68	0.46	0.26	350	15	1809	61
148.496	68.327	1607	1898	0.90	3.96	0.45	0.36	16	14	1814	1588	1898	1.00	4.08	0.52	0.39	17	13	1787	27
148.490	68.301	1721	2089	0.80	2.88	0.27	0.41	338	20	1953	1692	2090	0.90	3.12	0.29	0.37	337	20	1916	37
148.479	68.306	1670	2139	1.20	5.28	0.72	0.32	344	12	1958	1652	2139	1.30	5.40	0.75	0.32	341	13	1916	42
148.478	68.429	1702	2230	1.20	4.20	0.59	0.42	12	17	1954	1635	2230	1.40	4.92	0.71	0.37	21	16	1861	93
148.456	68.413	1736	1951	0.80	2.76	0.36	0.59	9	12	1861	1702	1951	0.90	3.12	0.40	0.51	13	12	1835	26
148.451	68.266	1621	2054	1.30	5.16	0.79	0.37	339	13	1845	1608	2055	1.40	5.40	0.85	0.37	337	13	1794	51
148.441	68.292	1638	1881	1.30	5.40	0.83	0.36	342	9	1786	1572	1881	1.80	6.84	1.07	0.29	338	8	1729	57
148.424	68.280	1692	1929	0.80	3.00	0.38	0.53	48	13	1799	1622	1929	1.00	3.36	0.48	0.53	51	13	1785	14
148.417	68.306	1583	1803	0.80	2.88	0.24	0.36	344	13	1679	1573	1803	1.00	3.24	0.31	0.37	355	10	1643	36
148.415	68.271	1590	1976	1.30	5.64	1.00	0.40	41	10	1863	1549	1976	1.30	6.12	1.06	0.36	41	10	1833	30
148.380	68.296	1622	1980	1.10	4.20	0.59	0.42	345	14	1852	1573	1980	1.40	4.80	0.71	0.39	343	13	1801	51
148.379	68.409	1680	2161	1.30	4.56	0.46	0.28	355	13	1863	1612	2161	1.60	5.04	0.60	0.30	359	12	1807	56
148.353	68.291	1663	1997	1.40	4.68	0.76	0.43	41	11	1864	1598	1998	1.60	5.52	0.83	0.34	44	11	1830	34
148.337	68.315	1640	2112	1.40	5.28	0.61	0.27	356	14	1823	1624	2111	1.70	6.24	0.79	0.25	348	11	1726	97
148.301	68.320	1642	1995	1.60	5.40	0.69	0.30	26	10	1817	1617	1995	1.60	5.76	0.75	0.28	29	10	1781	36
148.290	68.357	1669	1809	0.70	2.64	0.27	0.48	353	9	1752	1635	1810	1.00	3.36	0.39	0.43	359	8	1719	33

APPENDIX
Continued.

		Modern									Little Ice Age									
Longitude (°W)	Latitude (°N)	Minimum elevation (m)	Maximum elevation (m)	Length (km)	Perimeter (km)	Area (km^2)	Compact-ness[a]	Aspect from (0°)	Slope (degree)	ELA (m)	Minimum elevation (m)	Maximum elevation (m)	Length (km)	Perimeter (km)	Area (km^2)	Compact-ness[a]	Aspect from (0°)	Slope (degree)	ELA (m)	ΔELA (m)
148.254	68.357	1614	2263	1.60	7.92	1.24	0.25	339	11	1845	1578	2263	1.60	8.16	1.39	0.26	342	11	1785	60
148.232	68.376	1680	2247	1.60	5.76	0.78	0.30	7	13	1965	1615	2247	1.70	6.72	0.90	0.25	16	12	1882	83
148.219	68.348	1657	2105	1.30	5.52	0.85	0.35	5	11	1801	1627	2105	1.40	6.00	0.98	0.34	15	10	1780	21
148.210	68.372	1652	2001	1.40	4.20	0.55	0.39	350	11	1844	1566	2001	1.70	5.04	0.72	0.36	356	11	1776	68
148.178	68.337	1607	2121	1.40	8.88	1.13	0.18	33	13	1927	1446	2121	1.40	10.20	1.27	0.15	28	13	1829	98
148.178	68.376	1636	2218	1.60	7.32	1.11	0.26	4	10	2015	1636	2219	1.70	7.44	1.22	0.28	11	10	1940	75
148.147	68.462	1631	2267	1.40	6.48	0.85	0.25	0	16	1992	1590	2267	1.40	7.32	0.95	0.22	4	14	1847	145
148.111	68.446	1763	2250	1.30	4.44	0.47	0.30	269	15	1962	1710	2250	1.40	4.68	0.52	0.30	268	15	1890	72
148.106	68.349	1701	2102	0.90	3.00	0.31	0.43	17	20	1903	1654	2103	0.90	3.60	0.36	0.35	13	18	1855	48
144.985	69.221	1504	2168	1.40	4.68	0.50	0.29	329	20	1973	1452	2166	1.40	5.52	0.57	0.23	335	19	1809	164
144.968	69.187	1767	2153	0.90	3.72	0.44	0.40	317	17	1993	1728	2155	1.10	4.20	0.50	0.36	300	17	1939	54
144.934	69.040	1676	2053	1.00	3.84	0.39	0.33	35	16	1805	1632	2389	1.20	4.44	0.50	0.32	337	12	1718	87
144.926	69.216	1474	2394	2.40	10.56	1.48	0.17	343	14	1921	1427	2051	2.60	11.88	1.86	0.17	40	15	1840	81
144.854	69.071	1846	2051	0.50	1.80	0.13	0.52	10	19	1962	1806	2053	0.70	2.16	0.18	0.48	16	18	1918	44
144.839	69.040	1700	2184	1.10	3.84	0.44	0.38	24	20	1996	1625	2191	1.40	4.80	0.53	0.29	30	19	1948	48
144.271	69.277	1862	2316	1.30	4.32	0.52	0.35	179	13	2142	1828	2286	1.40	4.68	0.58	0.33	181	13	2106	36
144.253	69.193	1695	2418	1.30	11.28	1.80	0.18	327	24	2128	1557	2415	1.50	12.24	2.06	0.17	323	23	2041	87
144.245	69.181	1689	2410	1.70	7.80	1.29	0.27	46	16	2044	1567	2408	1.90	8.64	1.52	0.26	51	16	1972	72
144.164	69.271	1832	2385	1.00	5.04	0.49	0.24	72	21	2055	1816	2384	1.10	5.28	0.59	0.27	81	20	1998	57
144.075	69.229	1646	2196	1.50	5.04	0.66	0.32	347	18	1887	1540	2239	2.30	7.32	0.92	0.22	1	15	1825	62
143.918	69.226	1842	2307	0.90	4.56	0.59	0.35	303	19	2141	1766	2309	1.10	5.16	0.65	0.31	298	19	2098	43
143.877	69.320	1774	2022	0.90	3.12	0.35	0.45	5	13	1930	1740	2043	0.90	3.12	0.42	0.54	16	13	1899	31
143.833	69.267	1651	2432	3.00	12.36	2.15	0.18	316	14	2118	1603	2433	3.20	12.48	2.25	0.18	313	14	2045	73
143.788	69.070	1743	2198	1.10	6.60	0.65	0.19	330	18	2092	1620	2199	1.30	7.56	0.76	0.17	325	17	1973	119
143.776	69.192	1778	2205	0.90	3.84	0.41	0.35	28	15	2009	1691	2493	2.00	9.60	1.75	0.24	5	16	1994	15
143.741	69.286	1361	2396	2.80	21.36	3.59	0.10	28	11	2060	1337	2394	3.10	21.96	3.81	0.10	32	11	1950	110
143.740	69.178	1791	2173	0.60	2.28	0.18	0.43	25	22	2181	1729	2587	1.80	10.08	1.27	0.16	355	23	2075	106
143.738	69.219	1545	2587	1.80	9.24	1.17	0.17	351	23	2143	1494	2175	1.80	3.00	0.21	0.29	23	21	1972	171
143.730	69.306	1779	2067	1.10	3.60	0.45	0.44	36	11	1990	1745	2077	1.10	3.84	0.51	0.43	45	12	1966	24
143.702	69.209	2054	2248	0.40	1.20	0.07	0.60	6	29	2142	1666	2589	2.50	9.84	2.05	0.27	86	14	2129	13
143.552	69.130	1724	2342	1.40	6.00	0.79	0.28	352	13	2189	1681	2314	1.70	6.36	0.86	0.27	355	13	2101	88
143.492	69.110	1663	2372	2.30	10.08	2.59	0.32	2	13	2095	1625	2367	2.30	10.44	2.63	0.30	2	13	2056	39

[a] A nondimensional measure of circularity ranging from 0.0 for a straight line to 1.0 for a circle ($4\pi A/P^2$, where A = area and P = perimeter).